HHS Public Access

Author manuscript

Science. Author manuscript; available in PMC 2017 September 12.

Published in final edited form as:

Science. 2017 April 07; 356(6333): . doi:10.1126/science.aai8236.

Causal role for inheritance of H3K27me3 in maintaining the OFF state of a Drosophila HOX gene

Rory T. Coleman[1] and **Gary Struhl**[1,*]

[1]Department of Genetics and Development, Columbia University College of Physicians and Surgeons, 701 W 168th St., New York, NY 10032

Abstract

Many eukaryotic cells can respond to transient environmental or developmental stimuli with heritable changes in gene expression that are associated with nucleosome modifications. However, it remains uncertain whether modified nucleosomes play a causal role in transmitting such epigenetic memories, as opposed to controlling or merely reflecting transcriptional states inherited by other means. Here, we provide *in vivo* evidence that H3K27 trimethylated nucleosomes, once established at a repressed *Drosophila* HOX gene, remain heritably associated with that gene and can carry the memory of the silenced state through multiple rounds of replication, even when the capacity to copy the H3K27me3 mark to newly incorporated nucleosomes is diminished or abolished. Hence, in this context, the inheritance of H3K27 trimethylation conveys epigenetic memory.

Introduction

Animal development depends on the capacity of cells to choose particular fates in response to transient cues and for their descendants to inherit these decisions in the form of transcriptionally ON (activated) or OFF (silenced) states of gene expression. Unlike heritable changes in gene expression that result from alterations in DNA sequence, the primary mechanisms that operate during development are epigenetic, associated with the establishment of trans-acting, auto-regulatory circuits (1, 2) or cis-acting modifications of DNA or chromatin (3–5). Here, we address the question of whether the inheritance of cis-acting modifications of chromatin can play a causal role in the transmission of epigenetic memory. We focus on the potential role of histone H3 lysine 27 trimethylation (H3K27me3) as a cis-acting epigenetic mark (6) that controls the specification of body segments via the heritable silencing of HOX genes (7–10).

The evolutionarily conserved Polycomb group proteins, which function in Polycomb Repressive Complexes (PRCs), control the development of the animal body plan by repressing the transcription of critical regulatory genes, most notably the HOX genes, which dictate segment type (4–8). One such complex, PRC2, is responsible for catalyzing H3K27me3 (11–14). Both loss of PRC2 (8–10), as well as the replacement of wildtype H3 with modified versions that cannot be H3K27 trimethylated (15, 16), result in the failure to

*Correspondence to: gs20@columbia.edu.

maintain the OFF state of HOX genes. Similarly, HOX genes that lack cis-acting Polycomb Response Elements (PREs) required to recruit PRC2 fail to maintain the OFF state (17–19). These results establish the essential roles of PRC2 and H3K27me3 in HOX gene repression, but leave unanswered whether H3K27me3 functions as a heritable, epigenetic mark that confers the memory of the OFF state (20–23). To address this question, we used a transgenic form of the classic Drosophila HOX gene *Ultrabithorax* (*Ubx*) that allows us to assay persistence of the OFF state as well as H3K27me3 following PRE excision. Our results argue that once H3K27me3 nucleosomes are established at a HOX gene, they remain stably associated with the gene for the remainder of development, subject only to dilution by newly incorporated, naïve nucleosomes accompanying each subsequent replication cycle. Further, by manipulating the capacity of the newly incorporated nucleosomes to be trimethylated by PRC2, we alter the rate of dilution of H3K27me3 and demonstrate a causal relationship between the inheritance of the modification and the memory of the OFF state.

A PRE excision paradigm

Although native *Ubx* spans over 70Kb, *Ubx-lacZ* (*UZ*) mini-genes that recapitulate almost normal expression can be reconstituted using the promoter and three *Ubx* cis-acting regulatory elements: (i) an early enhancer (EE) for activating the ON state, (ii) a late, imaginal “disc” enhancer (DE) for maintaining the ON state, and (iii) a PRE to maintain the OFF state in the descendants of cells in which the gene was not initially activated (17, 18, 24, 25) (Methods). To analyze the role of H3K27me3 in the inheritance of the OFF state, we generated a *>PRE>UZ* transgene in which the PRE is embedded in a “Flp-out” cassette (26) that carries both the PRE as well as a ubiquitously expressed reporter gene, *Tub.CD2* (Fig. 1A; Methods). Transient expression of Flp under heat shock control generates $>UZ^{\Delta PRE}$ cells that lack the PRE and no longer express CD2, allowing us to monitor the consequences of PRE excision on the inheritance of both the OFF state and H3K27me3 in their clonal descendants.

Early roles of the PRE

Most genomic insertions of the *>PRE>UZ* transgene generate a pattern of β–Galactosidase (henceforth UZ) similar to that of endogenous Ubx throughout development, except restricted to parasegments 6–12, rather than parasegments 5–13 (Fig. 1B; Methods). The anterior boundary of parasegment 6 (PS6) subdivides the third thoracic segment, including the embryonic primordia of the imaginal discs that will give rise to the halteres of the adult fly, into abutting anterior (A) and posterior (P) compartments. Hence, *>PRE>UZ* is ON in the P compartment but OFF in the A compartment of this disc, as well as being OFF in the entire wing disc (which derives from the second thoracic segment; Fig. 1D).

As expected, the *>PRE>* cassette is required for the OFF state of the *>PRE>UZ* transgene, as zygotes carrying $>UZ^{\Delta PRE}$, the PRE-excised form of the transgene (Fig. 1A), give rise to animals that express UZ ubiquitously, both in embryos and in the imaginal discs (Figs. 1C,E). Unexpectedly, however, the $>UZ^{\Delta PRE}$ transgene is not activated in blastoderm stage embryos, in contrast to the intact *>PRE>UZ* transgene (Figs. 1B,C, left panels) as well as native *Ubx*. Instead, $>UZ^{\Delta PRE}$ expression is first detected only later, in extended germ band

embryos, where it is expressed ubiquitously (Figs. 1B,C, middle and right panels). Hence, the PRE is normally required in parasegments 6–12 to initiate the ON state, in contrast to its requirement for maintaining the OFF state in the remaining parasegments. Analysis of an *>EE>UZ* transgene in which the EE rather than the PRE is embedded in the cassette, confirms a coincident, early requirement for the EE in activating the ON state (Figs. S1A–F). Significantly, when this transgene lacks the *>EE>* cassette, the resulting OFF state depends on continuous PRC2 activity (Fig. S1G), and by inference, on the PRE. Thus, in early embryos, the EE and PRE are required together to initiate the ON state in parasegments 6–12, whereas the OFF state is established by default in the remaining parasegments and requires PRE anchored PRC2 for its subsequent maintenance.

Persistence of silencing following PRE excision

Previous studies have shown that PRE excision can result in the loss of transgene silencing in the wing disc, establishing a persistent requirement for PREs in maintaining the OFF state (27, 28). However, the *>PRE>* cassettes used in these studies did not carry marker transgenes, leaving unresolved whether release from silencing depends on the passage of time or cell division, or if it varies as a function of cell position. In contrast, inclusion of the *Tub.CD2* reporter gene inside the cassette in the *>PRE>UZ* transgene allows us to identify the clonal descendants of cells in which excision occurred and hence, to determine how release from silencing depends on these parameters.

We focus on the wing disc, where the *>PRE>UZ* transgene is uniformly OFF or ON depending on whether the PRE is present or absent, respectively, at fertilization (Figs. 1D,E). The disc is composed of a thick columnar epithelium subdivided into three domains destined to form the prospective notum (body wall), hinge, and wing blade, as well as an opposing squamous epithelium of peripodial cells (Fig. 2A). The columnar domains are also partitioned into antero-posterior (A/P) and dorso-ventral (D/V) compartments, as well as additional subdomains, by various transcription factors that control their region-specific fates (29).

To assay the consequences of removing the PRE, we induced excision of the *>PRE>* cassette at chosen times and assayed UZ expression in the resulting $>UZ^{\Delta PRE}$ clones, marked by the absence of CD2 expression, at the end of larval life (120 hours after egg laying (AEL); Fig. 2A). Surprisingly, release from silencing in such clones varies dramatically, depending on cell position and the timing of clone induction. $>UZ^{\Delta PRE}$ clones generated shortly after gastrulation (6–9 hrs AEL) express UZ cell-autonomously, regardless of position within the disc (Fig. 2B). However, clones induced later in embryogenesis (18 hrs AEL) do not express UZ in portions of the prospective notum; clones induced during the second to early third larval instar (48–72 hrs AEL) fail to express UZ in the remainder of the notum and much of the wing hinge; clones induced during the mid-third larval instar (96 hrs AEL) escape silencing only along the D/V compartment boundary in the hinge and wing blade; finally, clones induced in the late third instar (108 hrs AEL) derepress UZ only in the peripodial cells. Importantly, whether $>UZ^{\Delta PRE}$ cells generated at any given time remain silenced depends only on their location within the disc and not their clonal history, as release from silencing depends on cell position even within single, isolated clones (Fig. S2).

These results are unexpected and show that release from silencing following PRE excision varies over a remarkable range, extending from as little as 12 hours (peripodial cells) to as long as 4 days (notum). Hence, we infer (i) that the level of repression associated with the PRE confers a barrier that is normally sufficient to silence the *UZ* promoter, but diminishes over time following PRE excision (e.g., due to lability of the H3K27me3 mark and/or its dilution during replication) and (ii) that the ability of enhancers within the transgene to override this decaying barrier varies depending on the different activating strengths of regionally-expressed transcription factors that would otherwise drive $>UZ^{\Delta PRE}$ expression (30, 31). In support, we observe that regions of the disc that show high levels of UZ expression in entirely $>UZ^{\Delta PRE}$ animals (e.g., the wing blade) exhibit a rapid loss of silencing following PRE excision, whereas those that show low level expression (e.g. the notum) exhibit a much slower loss (Fig. 1E). Similar temporal and spatial constraints have been observed for release of native *Ubx* from silencing following the removal of PRC2 (14, 30, 32), suggesting that they reflect a general property of *Ubx* silencing recapitulated by the transgene.

Cell division-dependent release from silencing

To determine whether release from silencing depends on the passage of time, or passage through a given number of cell divisions, we devised a strategy to assay the consequences of PRE excision in mitotically quiescent cells. To do so, we used a genetic approach to block pupation, creating larvae that develop at almost the normal rate until the imaginal discs reach mature size and cease proliferative growth, after which the larvae continue to feed and increase in body mass for up to three weeks (33, 34)(Methods). We then assayed the consequences of excising the PRE in the “stalled” discs of such larvae (Fig. 2C), focusing on the prospective wing blade where most cells normally release from silencing within 48–72 hrs (Fig. 2B).

PRE excision clones induced 72 hrs or longer before the stall show release from silencing in the wing blade, as in normal discs (Fig. 2B). In contrast, clones induced only ~24 hrs before the stall, or anytime thereafter, show no release even when assayed 2–3 weeks later (Fig. 2D). To test if the failure of such clones to release from silencing is due their having failed to undergo a requisite number of cell divisions, we ectopically expressed the signaling molecule Hedgehog (Hh), which causes A compartment cells located at a distance from the A/P compartment border to continue to divide after the stall. To do so, we used a Flp-out *Tub>y+>hh* transgene (35) to co-induce clones of *Tub>hh* cells at the same time that we generated PRE excision clones. When such $>UZ^{\Delta PRE}$ and *Tub>hh* clones are induced concomitantly during early larval life, all PRE excision clones grow extensively prior to the stall and show release from silencing in the prospective wing (Fig. 2E). In contrast, when such clones were co-induced only ~24 hrs before the stall, only A compartment clones away from the A/P boundary continue to proliferate after the stall, and only these clones show release from silencing (Fig. 2F). Hence, the OFF state of $>UZ^{\Delta PRE}$ expression can be maintained indefinitely in prospective wing cells following excision as long as proliferation is blocked within a few cell divisions. In contrast, wing cells that undergo additional divisions fail to maintain the OFF state.

We conclude that heritable silencing conferred by the PRE is stable to the passage of time but labile to cell division following PRE excision, with the number of cell divisions required for release from silencing in any given cell depending on its position within the disc.

Cell division-dependent dilution of H3K27me3

Our finding that release from silencing depends on cell division is consistent with the hypothesis that H3K27me3 nucleosomes can remain associated with the transgene locus for at least several cell generations following PRE excision and can perpetuate the OFF state until diluted sufficiently by the incorporation of unmodified nucleosomes during subsequent replication cycles. If correct, and if only PRE-anchored PRC2 can catalyze H3K27me3, PRE excision should result in at least a two-fold reduction in the level of H3K27me3 associated with the transgene following each round of replication (as observed for the cell-division dependent loss of parental genomic H3K27me3 (36–38)). However, if PRC2 that is not anchored at the PRE can also trimethylate H3K27, albeit at lower efficiency, the rate of dilution would be slower. To test if PRE excision results in replication coupled dilution of H3K27me3, and to assess the rate of dilution, we have used chromatin immunoprecipitation followed by quantitative PCR (ChIP-qPCR) to monitor H3K27me3.

In the wing disc, where native *Ubx* is OFF, the entire locus has high levels of H3K27me3 (39). The same is true for the silenced *Ubx* and *lacZ* encoding portions of the intact *>PRE>UZ* transgene, albeit not for the ubiquitously expressed, CD2 encoding portion of the *>PRE>* cassette (Fig. 3B, left panel, white data sets). In contrast, animals carrying the $>UZ^{\Delta PRE}$ form of the transgene show only background levels of H3K27me3 using the same probes (Fig. 3B, left panel, grey data sets; total histone H3 levels are similar for both the *>PRE>UZ* and $>UZ^{\Delta PRE}$ transgenes, right panel; see Table S1 for further quantitation and mock ChIP controls). Hence, all detectable H3K27me3 associated with the intact *>PRE>UZ* transgene depends on the presence of the *>PRE>* cassette.

To assay the consequences of PRE excision on the level of H3K27me3, we induced PRE excision clones at 24, 48, and 72 hours before the end of larval life and assayed the discs just prior to pupation (~120 hrs AEL; Fig. 3C). Since PRE excision was only ~55% efficient (Fig. S3), qPCR probes were designed that would detect only intact *>PRE>UZ* or PRE-excised $>UZ^{\Delta PRE}$ chromatin (IN or EX probes, respectively; Fig. 3A). Because IN and EX probes amplify different sequences, comparing the levels of H3K27me3 they detect is not informative. Instead, IN probes serve as an internal control for the consistency of H3K27me3 levels in cells in which PRE excision did not occur. Further, heat shock transiently perturbs both H3K27me3 and total H3 ChIP qPCR signals, precluding obtaining a “zero” time point for the EX probe. Hence, we focus on comparing H3K27me3 levels in discs in which PRE excision was induced 24, 48 and 72 hours before being assayed at 120 hrs AEL. Using the EX probe, we observed H3K27me3 signals of 7.9±2.3, 6.0±1.3, and 4.2±0.9 (mean of the % input ± SD), respectively, for the 24, 48 and 72 hr time points (Fig. 3C, left panel, grey data sets). These levels are all significantly above the 0.7±0.3 background detected by this probe in $>UZ^{\Delta PRE}$ wing discs (Fig. 3C, ΔPRE). In contrast, the levels of H3K27me3 observed using the IN probe were not significantly different for each of the three time points (Fig. 3C, left panel, white data sets; Table S2). Thus, following PRE

excision, the EX probe detects a progressive, albeit slow, decline in the level of H3K27me3 associated with *>UZ$^{\Delta PRE}$* chromatin, whereas the IN probe shows no significant change.

To test whether there is a causal relationship between cell division and the dilution of H3K27me3, we performed ChIP-qPCR analysis of wing discs obtained in the "stalled" disc paradigm (Fig. 2D). Specifically, PRE-excision was induced concomitant with the stall (144 hrs AEL) and ChIP was performed 24, 48, or 120 hours following excision (Fig. 3D). In contrast to actively dividing wing discs, we detect no significant dilution of either H3K27me3 or total H3 levels, even between the 24 and 120 hour time points (Fig. 3D; Table S3). Hence, we conclude that the progressive dilution of H3K27me3 observed in growing discs depends on cell division.

Finally, because cell division in the wing disc normally slows down towards the end of larval life (40), we used an *Actin5C>stop>lacZ^{nuclear}* lineage trace transgene (26) to determine that wing cells undergo an average of around 1, 3 and 6 cell divisions, respectively, during the last 24, 48 and 72 hours of disc growth and to confirm that wing and notum cells proliferate at similar rates (Fig. S4). This quantitation allows us to estimate that following PRE excision, H3K27me3 levels decline at a rate of ~10–12% per cell cycle. Hence, after five to six cell divisions, H3K27me3 of the *>UZ$^{\Delta PRE}$* transgene would be reduced by ~50%, which appears sufficient to allow release from silencing in the prospective wing blade, but not in the prospective notum. This rate of dilution is much lower than what would be expected for the simple scenario in which PRC2 must be anchored at the PRE to trimethylate H3K27, which would predict a 50% reduction after each replication cycle. Hence, we infer that some PRC2 that is not anchored at the PRE can contribute, even though this activity is not sufficient to stably maintain H3K27me3 over an indefinite number of cell generations.

H3K27me3 inheritance and epigenetic memory

Inheritance of H3K27me3 involves two distinct events: (i) transmission of parental H3K27me3 nucleosomes to daughter DNA during replication and (ii) propagation of the H3K27me3 mark from parental to newly incorporated naïve nucleosomes following replication. If inheritance, per se, is responsible for carrying the memory of the OFF state, then any manipulation that compromises either event should reduce the number of divisions required for release from silencing, with the reduction in the number of divisions required being determined by the extent to which inheritance of the mark is compromised. We have tested this prediction using two independent approaches.

In the first approach, we have compared PRE excision clones in animals in which all histone H3 molecules are wildtype ($H3^+$) versus clones generated in animals in which we spiked the $H3^+$ pool with a K27R mutant form of H3 that cannot be trimethylated at residue 27 ($H3^{K27R}$). To do so, we used larvae in which the native (and sole) histone gene complex (*HisC*) is replaced by multiple transgenic copies of histone genes, some of which encode wildtype $H3^+$ and others of which encode $H3^{K27R}$, to provide a chosen ratio of $H3^+$ to $H3^{K27R}$ (15, 16, 41). We focus on the prospective notum where clones generated by PRE excision during the first instar normally remain silenced for the rest of larval life (Figs. 2B, 4B, right panel) — a period of ~96 hours that our lineage trace and ChIP-qPCR data indicate should correspond to at least 8 cell divisions and a ~60–70% reduction in H3K27me3 levels.

If replacing the wildtype complement of histone H3 with a mixture of $H3^{K27R}$ and $H3^{+}$ results in fewer cell cycles being required for the release from silencing, we reasoned that this might be apparent in the notum where no release from silencing would otherwise occur.

Animals in which all histone H3 molecules derive from a 12:8 dosage of $H3^{+}$ to $H3^{K27R}$ encoding genes (henceforth 12K:8R) develop into viable and fertile flies albeit with mild homeotic transformations (e.g. ectopic sex combs on the second and third legs) and have ~30% lower H3K27me3 levels at the *>PRE>UZ* locus in the OFF state (Fig. 4A; left panel; Table S4). This level is similar to that observed in wild type wing disc cells after about three rounds of division following PRE excision. When present in this genetic background, the *>PRE>UZ* transgene shows virtually no expression in the columnar epithelium of the wing disc, the only exception being rare, small patches in the vicinity of the D/V compartment boundary (Fig. S5C, and below). Strikingly, when PRE excision is induced in such 12K:8R larvae during the first instar, we observe extensive release from silencing in the prospective notum at the end of larval life, in contrast to the failure to release from silencing observed in wildtype discs (Fig. 4B). Thus, spiking the $H3^{+}$ pool with $H3^{K27R}$ significantly reduces the number of cell divisions required for release from silencing after PRE excision, whether because the cells initially begin with a ~30% lower level of H3Kme3 or because the capacity of PRC2 to copy the mark has been compromised, or both.

To restrict our analysis to the effects of compromising only the copying activity of PRC2, we generated 12K:8R animals that carry both the *>PRE>UZ* transgene as well as a single copy of the wildtype *HisC locus*, which carries more than 100 copies of the native $H3^{+}$ gene, negating any deleterious effect that the 8 $H3^{K27R}$ genes might otherwise have (15). We then co-induced three kinds of clones: those that lack either the *HisC* locus, the *>PRE>* cassette or both (Methods). When generated during the first larval instar, clones that lack both — and only those clones — show cell autonomous release from silencing in the prospective notum (Fig. 4C). Hence, increasing the dilution rate of H3K27me3 by spiking the $H3^{+}$ pool with $H3^{K27R}$ is sufficient to cause a significant reduction in the memory of the OFF state, even in cells that begin with a virtually normal complement of $H3^{+}$ nucleosomes.

These results provide evidence for a causal relationship between inheritance of H3K27me3 and the memory of the OFF state, and are supported further by our findings that the intact *>PRE>UZ* transgene is expressed in rare, small patches in distal wing cells of 12K:8R discs and that loss of silencing is further accelerated in 6K:6R wing discs (as documented and discussed in Fig. S5C). However, they are subject to the criticism that this evidence has been obtained under conditions in which the capacity of PRC2 to copy K27me3 is systemically and persistently compromised by the presence of $H3^{K27R}$, albeit so slightly as to have virtually no detectable effect except in PRE excision clones.

To address this concern, we used a second, and independent, approach in which we transiently knocked down PRC2 activity for a period that is sufficiently brief as to have no detectable effect on silencing of the intact *>PRE>UZ* transgene, and then asked if this manipulation is sufficient to accelerate the decline in both H3K27me3 levels and the memory of the OFF state following PRE excision. To do so, we used the $Gal80^{ts}$/Gal4

method (42) to express an RNAi against *Enhancer of zeste* (*E(z)*), the catalytic component of PRC2 (11–14), under temperature control.

In the presence of Gal80^{ts}, Gal4 dependent expression of the *UAS.E(z)RNAi* transgene is blocked at 17°C, but induced at 29°C, and imaginal discs that are shifted from 17°C to 29°C for 36 hours or longer show release from silencing for both native *Ubx* and the *>PRE>UZ* transgene. However, silencing is stringently maintained in wing discs that are shifted to 29°C for only 24 hrs, whether assayed immediately after the 24 hr shift or any time thereafter. In this background, we induced PRE excision clones in second instar larvae maintained at 17°C that either did, or did not, carry the *UAS.E(z)RNAi* transgene and then immediately shifted them to 29°C for 24 hrs, followed by a return to 17°C for the remainder of larval development, at which time wing discs were assayed for both UZ expression and H3K27me3 (Fig. 5).

Transient expression of *E(z)RNAi* considerably shortened the memory of the OFF state following PRE excision relative to the no RNAi control, as indicated by the release from silencing in the notum (Fig. 5C). Similarly, it resulted in a ~2 fold further reduction in H3K27me3 levels relative to the no-RNAi control (down to 2.2±0.7 in *E(Z)RNAi* discs versus 5.2±2.3 for the control; Fig. 5B, EX probe; Table S5). This difference is consistent with a 50% dilution of H3K27me3 accompanying one cycle of replication in the absence of PRC2 — the expected maximum if all parental H3K27me3 nucleosomes are inherited but no copying of the H3K27me3 mark occurs — after which the rate of dilution would return to 10–12% (as measured in wildtype discs in Fig. 3C). We note that H3K27me3 levels also declined, albeit modestly in cells that did not lose the PRE (from 10.6±1.6 to 8.3±1 in control versus *E(Z)RNAi* discs, respectively; Fig. 5B, IN probe, Table S5), raising the possibility that it might take a few cell cycles following the restoration of PRC2 activity for the level of H3K27me3 of the intact *>PRE>UZ* transgene to recover fully following a transient two-fold depletion.

H3K27me3 inheritance and native *Ubx* silencing

To assess how our PRE excision experiments relate to heritable silencing of native *Ubx*, we monitored the loss of *Ubx* silencing after abruptly abolishing the capacity of PRC2 to trimethylate newly synthesized histone H3 molecules.

To do so, we created single daughter cells that express only the H3^{K27R} mutant form of histone H3, but derive from mother cells that have a virtually wildtype complement of H3^{+} nucleosomes (15, 16) (Methods). Under these conditions, the sole supply of H3^{+} nucleosomes that can carry the H3K27me3 mark in subsequent cell generations derives from the mother cell, resulting in at least a two-fold dilution of the starting level of H3K27me3 with each subsequent replication cycle. The clones generated from such daughter cells show a rapid loss of *Ubx* silencing, within 24–36 hours in the prospective wing (~1 division following the division required to generate the mutant daughter cell and a predicted ~2 fold dilution in H3K27me3) and within 48 hours in the prospective notum (~1–2 further divisions and a further ~2–4 fold dilution) (Fig. S6). Although approximate, these estimates suggest that similar position-dependent declines in the levels of H3K27me3 are required to cause release from silencing of both *Ubx* and the *>PRE>UZ* transgene (> ~2 fold in the

prospective wing and > ~4–8 fold in the prospective notum; Fig. 6B). Hence, the causal relationship between inheritance of H3K27me3 and memory of the OFF state appears to be similar for both the transgene and native *Ubx*.

Discussion

Despite the ubiquity with which diverse chromatin modifications have been associated with either stasis or change in the transcriptional behavior of eukaryotic genes, the question of whether any such modifications have a causal role in epigenetic memory remains controversial (20, 21, 43, 44). Here, we provide evidence that silencing of the paradigmatic Drosophila HOX gene *Ubx* by H3K27me3 provides an example of a chromatin modification that executes just such a causal role in the propagation of epigenetic memory.

First we confirm and extend previous evidence (45) that the ON state is initiated under the transient control of an early enhancer (EE). We do so by showing that once the ON state of a *Ubx-lacZ* (*UZ*) transgene is established by EE activity, it is sustained in all descendant cells, even if the EE is subsequently excised.

Second, we show that in the absence of EE activity, the *UZ* transgene adopts the OFF state and maintenance of this state now depends, by default, on Polycomb Repressive Complex 2 (PRC2), the methyltransferase that catalyzes H3K27me3 (11–14).

Third, we confirm and extend previous evidence (17–19, 27, 28) that maintenance of the OFF state depends on a Polycomb Response Element (PRE), which anchors PRC2 in the vicinity of the *Ubx* locus. We do so by showing that excision of the PRE results in the loss of H3K27me3 and release from silencing.

Fourth, we show that both the loss of H3K27me3 as well as the release from silencing depend on cell division. If division is blocked, neither occurs and the OFF state can persist indefinitely; if division continues, H3K27me3 is diluted with each subsequent replication cycle and silencing is lost.

Fifth, we establish a causal relationship between cell division-dependent dilution of H3K27me3 and the memory of the OFF state. Manipulations that accelerate the rate of dilution reduce the number of cell divisions required for the release from silencing (Fig. 6B).

It has been proposed that inheritance of H3K27me3 depends on two mechanisms: (i) the local re-deposition of parental H3K27me3 nucleosomes following replication, and (ii) the capacity of these modified parental nucleosomes to serve as templates for PRC2 to copy the H3K27me3 mark onto newly incorporated nucleosomes (46–48). If PRC2 must be recruited by the PRE to copy the mark, PRE excision should result in a 50% reduction in H3K27me3 levels following each subsequent replication cycle. However, we observe a much slower rate of decline of ~10–12%. Hence, we infer a significant contribution of PRC2 that is not anchored at the PRE (henceforth “free” PRC2). In support, we can negate this contribution by knocking down total PRC2 activity.

The physical association of PRC2 with chromatin is highly dynamic in vivo, with free PRC2 rapidly exchanging with chromatin bound PRC2 (49). Hence, as diagrammed in Fig. 6A, we envisage the PRE as a recruiting center that sustains a high, local concentration of PRC2 that is necessary for efficient copying of the H3K27me3 mark. According to this view, PRE excision should reduce the local availability of PRC2, allowing some of the nucleosomes that were incorporated following replication to escape being H3K27 trimethylated and resulting in the serial dilution of H3K27me3 nucleosomes during subsequent cell cycles.

Thus, we posit that once the OFF state of HOX gene expression is initially established by a transient transcriptional repressor (45), it can be — and normally is — perpetuated indefinitely via transmission of parental H3K27me3 and copying of the H3K27me3 mark (Fig. 6A). However, indefinite inheritance of the mark, and hence stable memory of the OFF state, requires the PRE to ensure that the mark is efficiently copied after each replication cycle. This memory function is distinct from transcriptional repression of genes bearing the mark (30), which depends on a second, chromatin modifying, Polycomb Repressive Complex (PRC1) that is recruited at least in part by its capacity to bind directly to H3K27me3 (50–52).

Our results have three additional implications. First, we have discovered, unexpectedly, that the number of cell divisions required to release the *UZ* transgene from silencing after PRE excision depends on cell position. The range extends from ~1–2 cell divisions (peripodial cells) to ~3–5 cell divisions (wing) to >8 cell divisions (notum) and appears to correlate with the position-dependent level of expression in entirely $>UZ^{\Delta PRE}$ animals, which we infer reflects the different activating strengths of transcription factors that would otherwise act on the *UZ* promoter in different regions of the disc. Hence, we posit (i) that repression conferred by H3K27me3 is normally sufficient to hold all these position-dependent, activating inputs at bay, and (ii), that after PRE excision, the subsequent, serial dilution of H3K27me3 results in release from silencing wherever the local activating inputs are sufficiently strong to breach the decaying repressive barrier. Based on this reasoning, we suggest that many of the hundreds of Drosophila genes associated with PREs and H3K27me3 (31, 53) may not be heritably activated or silenced by PRE/PRC2 activity. Instead, PRE/PRC2 dependent repression may be counterbalanced by, and integrated with, activation by enhancers at these loci. By contrast, HOX genes may belong to a special class that has been stringently selected to exclude enhancers that can override PRE/PRC2 repression — a prerequisite for their essential roles as heritable determinants of segmental fate.

Second, for H3K27me3 nucleosomes to serve as carriers of epigenetic memory, they must remain stably associated with the loci they regulate, being copied along with the associated DNA from one cell generation to the next. Although it has been argued that nucleosome exchange, demethylation, and other nucleosome modifications might constrain the capacity of H3K27me3 nucleosomes to carry epigenetic memory (20, 21), our results argue that these constraints do not apply, in vivo, to *Drosophila* HOX genes. This is consistent with recent evidence suggesting little if any role for the sole *Drosophila* H3K27me3 demethylase Utx in HOX gene regulation after embryogenesis (54), as well as a low rate of nucleosome turnover at repressed HOX loci in cell culture (55, 56). Likewise, it has been reported that all

nucleosomes deposited behind the replication fork initially lack the H3K27me3 mark (57, 58), leading to the proposal that parental PRC components that remain anchored at the PRE are responsible for subsequently reestablishing the mark (57), and are thus, the actual mediators of epigenetic memory. This possibility, however, would predict that PRE excision should result in the loss of silencing following the first round of replication, a prediction that is directly contradicted by our findings and inconsistent with related studies (59, 60).

Third, our findings pose the question of whether chromatin modifying enzymes associated with epigenetic memory need to be anchored at *cis*-acting DNA elements, or if they can be recruited solely by their capacity to bind pre-existing modifications on parental nucleosomes. Recent studies in yeast have established that transient targeting of the H3K9 methyltransferase Clr4 to a reporter gene can suffice to initiate an epigenetic OFF state that is propagated indefinitely after the targeting agent is removed (*61, 62*). However, long term perpetuation of the mark is only observed under non-physiological conditions in which an opposing demethylase, Epe1, is eliminated.

In the case of PRC2 and H3K27me3, our results indicate that the PRE is required for long term, epigenetic memory. Nevertheless, PRC2 can perpetuate the mark and sustain the OFF state for at least eight cell generations following PRE excision, raising the possibility that free PRC2 can propagate the mark, albeit sub-optimally, in the absence of a PRE anchor. However, a more rapid loss of silencing has been observed for more minimal PRE-excision transgenes composed of heterologous promoters and/or enhancers (28). Hence, the slower rate exhibited by the *>PRE>UZ* transgene may reflect the presence of one or more *cis*-acting elements that help retain local PRC2 activity following PRE excision. These elements could be cryptic PRC2 anchors, but if so, they differ from canonical PREs in lacking the capacity to mediate H3K27me3 and maintain the OFF state on their own (e.g., in $>UZ^{\Delta PRE}$ animals; Figs. 1C,E;3B). Alternatively, they might target the $>UZ^{\Delta PRE}$ transgene to sub-nuclear domains such as Polycomb bodies where other PRC2 repressed loci congregate (63), or allow H3K27me3 to spread over a larger extent of the surrounding chromatin. Either of these latter possibilities might increase the local concentration of PRC2 via its capacity to bind, albeit only weakly, to resident H3K27me3 nucleosomes, and hence, might help compensate for the loss of the PRE.

In sum, our findings establish H3K27me3 as a chromatin modification that can function as a bona fide carrier of epigenetic memory. The capacity of H3K27me3 to function in this way is qualified by context — in the case of Drosophila HOX genes, by the requirement for cis-acting PREs, the absence of an opposing demethylase, and evolutionary constraints that exclude the emergence of enhancers that can override H3K27me3 mediated repression. Nevertheless, it provides a precedent for a physiologically significant role for chromatin modification in epigenetic inheritance.

Materials and Methods

Constitution and characterization of the *>PRE>UZ* and *>EE>UZ* transgenes

The *>PRE>UZ* and *>EE>UZ* transgenes are diagrammed in Figures 1 and S1 and were constructed by standard recombinant DNA technology using the Carnegie 2 P-element

vector and previously defined genomic fragments from the *Ubx*, *y*, and *Tuba1*genes, as well as a Flp-out cassette containing the Rat CD2 coding sequence (see Table S6 for a listing of the sequences defining the ends of each fragment; a full sequence of the both transgenes is available on request). The PRE is the well defined 1.6Kb *bxd* PRE. The EE is the similarly well defined 0.6Kb *pbx* early enhancer, which is activated in parasegments 6–12 (18, 24). Expression of native *Ubx* in parasegment 5 depends on *abx*/*bx* enhancers (64, 65), which are not present in our construct. Both transgenes were introduced into the genome by P-element mediated transformation, identified by virtue of rescue of the *y* mutant phenotype, mapped by standard genetic means, and the sites of insertion determined by inverse PCR (*66*). 4/7 genomic insertions of the *>PRE>UZ* transgene were expressed like previously described *Ubx-lacZ* transgenes (24, 25) and behaved similarly following excision of the *>PRE>* cassette: we focused our analysis on a single insert at 55B11. The remaining 3/7 genomic insertions were influenced in different ways by neighboring genomic DNA and will be described elsewhere. Similarly, 2/2 genomic insertions of the *>EE>UZ* transgene were expressed like previously described *Ubx-lacZ* transgenes and behaved similarly following excision of the *>EE>* cassette: we focused our analysis on a single insert at 92A13.

Experimental genotypes

Transgenes and mutant alleles are indicated by Bloomington or VDRC stock number or described in Flybase or prior publications. We are especially grateful to Vince Pirrotta, for the esc^{6} $escI^{-}$ double mutation, Jürg Müller for the *Df(2L)HisC*, $3XHisGU^{wt}$ $3XHisGU^{wt}$ and $3XHisGU^{K27R}$ $3XHisGU^{K27R}$ transgenes, Dan McKay for the $12XHis^{wt}$ and $8XHis^{H3K27R}$ transgenes, Henry Krause for the *phm.Gal4* and *UAS.fh-RNAi* transgenes, and Joe Parker for the *phm.LexA* and *LexO.fhRNAi* transgenes

hsp70.flp, *tub>y*$^{+}$*>hh*, *Act>Draf+>nuc-lacZ*, (26, 35)

$tub.Gal80^{ts}$ (Bloomington #7108)

hdc.Gal4 (expressed in all imaginal disc cells; (*67*))

Tub.Gal4, *UAS.GFPnls*, and *Tub.Gal80* (*68, 69*)

esc^{6} $escI^{-}$ (*70*)

UAS.E(z)RNAi (Bloomington #36068)

UAS.dcr (Bloomington #24648)

UAS.fhRNAi and *phm.Gal4* (33, 34)

phm.LexA and *LexO.fhRNAi* (gift of Joe Parker)

Df(2L)HisC (41)

$12XHis^{wt}$ (15)

$8XHis^{H3K27R}$ (15)

$3XHisGU^{wt}$ $3XHisGU^{wt}$ (16)

$3XHisGU^{K27R}$ $3XHisGU^{K27R}$ (16)

Ubi.GFP (Bloomington #5189)

The exact genotypes are indicated below, by Figure

1B&D, 2B, 3B&C, S2, S3, S4A&B: *y w hsp70.flp; >PRE>UZ/+*

1C&E, 3B&C, S1A, S3, S4A&B: *y w hsp70.flp; >UZ$^{\Delta PRE}$/+*

2D: *y w hsp70.flp UAS.dicer; >PRE>UZ/UAS.fhRNAi; phm.Gal4/+*

2E&F: *y w hsp70.flp UAS.dicer; >PRE>UZ/tub>y^{+}>hh UAS.fhRNAi; phm.Gal4/+*

3D: *y w hsp70.flp; >PRE>UZ/+; phm.LexA/LexO.fhRNAi*

4A&B, S5C: *y w hsp70.flp; Df(2L)HisC FRT40 >PRE>UZ/ Df(2L)HisC FRT40; 12XHis^{wt}/12XHis^{wt}*

4A&B, S5C: *y w hsp70.flp; Df(2L)HisC FRT40 >PRE>UZ/ Df(2L)HisC FRT40; 12XHis^{wt}/8XHis^{H3K27R}*

4C: *y w hsp70.flp; Df(2L)HisC FRT40 >PRE>UZ / Ubi.GFP FRT40; 12XHis^{wt}/ 8XHis^{H3K27R}*

5B&C: *y w hsp70.flp; tub.Gal80^{ts} >PRE>UZ/+; hdc.Gal4/+*

5B&C: *y w hsp70.flp; tub.Gal80^{ts} >PRE>UZ/UAS.E(z) RNAi; hdc.Gal4/+*

S1B,D&F: *y w hsp70.flp; >EE>UZ/+*

S1C&E: *y w hsp70.flp; >UZ$^{\Delta EE}$/+*

S1G: *y w hsp70.flp Tub.Gal4 UAS.GFPnls; esc^{6} escl· FRT40 / Tub.Gal80 FRT40; >UZ$^{\Delta EE}$/+*

S4B-D: *y w hsp70.flp; Act5c>Draf^{+}>lacZ/+*

S5A&B: *y w hsp70.flp; Df(2L)HisC FRT40 >PRE>UZ/Df(2L)HisC FRT40; 3XHisGU^{wt} 3XHisGU^{wt}/3XHisGU^{wt} 3XHisGU^{wt}*

S5A-C: *y w hsp70.flp; Df(2L)HisC FRT40 >PRE>UZ/Df(2L)HisC FRT40; 3XHisGU^{wt} 3XHisGU^{wt}/3XHisGU^{H3K27R} 3XHisGU^{H3K27R}*

S6: *y w hsp70.flp; Df(2L)HisC FRT40 >PRE>UZ/Ubi.GFP FRT40; 8XHis^{H3K27R}/ 8XHis^{H3K27R}*

Generation and immuno-staining of clones in wing imaginal discs

"Flp-out" cassette excision, Flp/FRT mediated mitotic recombination and the MARCM techniques were performed as previously described (26, *68, 71*). Timing of heat shock induced Flp activity is indicated in the text and relevant Figures.

Care was taken to ensure optimal growth conditions and accurate timing between PRE excision and processing for antibody staining or ChIP-qPCR analysis (e.g., necessary to resolve previously unrecognized differences (15) in the kinetics of release from silencing of native *Ubx* in H3^{K27R} clones, as in Fig. S6).

For PRE excision experiments, patches of cells lacking CD2 expression were only observed when animals carrying the *>PRE>UZ* transgene were heat shocked in the presence of a *hsp70.flp* transgene. Moreover, the frequency, size and distribution of such clones were similar to that of standard linear trace, Flp-out transgenes (such as *Act5c>Draf*$^{+}$*>lacZ*; Fig. S4; below), including in the haltere disc, where the UZ promoter is heritably silenced in the A compartment, but expressed in the P compartment. Hence, the presence of the PRE does not adversely affect either *>PRE>* excision or expression of the *Tub.CD2* mini-gene within the *>PRE>* cassette, even in cells in which it maintains the OFF state of the *>PRE>UZ* transgene. Accordingly, loss of CD2 expression is an independent, cell-autonomous marker of PRE excision.

Wandering, late third instar larvae were dissected and fixed in 4% paraformaldehyde. Wing discs were stained with the following primary antibodies: mouse anti-Rat CD2 (1:2,000; BD Parmingen#OX-34), rabbit anti-β-gal (1:20,000; Cappel), Rat αHb (MacDonald, 1/4000), Guinea Pig αDll (Richard Mann; 1/6000), mouse anti-Ubx (1:50; DSHB#FP3.38), mouse anti-GFP (1:2,000; DSHB#12A6), mouse anti-Wg (1:30; DSHB#4D4). Fluorescently-conjugated Alexa-Fluor secondary antibodies (ThermoFisher) plus Hoechst 33342 (Invitrogen) were used for visualization and discs were mounted in Vectashield medium (Vector). We thank Paul Macdonald and Richard Mann for the αHb and αDll antisera.

Chromatin Immunoprecipitation

For all ChIP experiments the following procedure was performed four times to produce four independent biological replicates (represented by individual data points in ChIP graphs). The only exception is in Figure 4A, where one of the 12K:8R replicates was lost in processing. All ChIP experiments were performed on wing discs from wandering, late third instar larvae, just prior to pupation.

To ensure larvae were of the same approximate stage, embryos were collected from fly cages in 4 hour intervals and the larvae from these collections were grown at 25°C at low density to avoid competition. 35 larvae were dissected at 116–120 hours AEL for each ChIP experiment and were fixed as follows: 25min; 1.8% paraformaldehyde in 50mM HEPES + 1mM EDTA + 0.5mM EGTA + 100mM NaCL. As per Estella et al. (*72*), following fixation, samples were quenched (6 min; 0.125M glycine in PBS + 0.01% TritonX100) and put through a series of washes in the presence of Complete Mini EDTA-Free protease inhibitor (denoted PI; Roche): two 10 min. washes in Buffer A (10mM HEPES + 10mM EDTA + 0.5mM EGTA + 0.25% TritonX100 + PI) followed by two 10 min. washes in Buffer B (10mM HEPES + 1mM EDTA + 0.5mM EGTA + 200mM NaCl + 0.01% TritonX100 + PI). Individual wing discs were then dissected from carcasses in Buffer B. Wing discs for individual biological replicates were pooled, transferred to sonication buffer (10mM HEPES + 1mM EDTA + 0.5mM EGTA), and sonicated on ice. For each sample, the chromatin was split according to the number of antibodies being used for ChIP and 10% of the sample chromatin was removed for use as the input sample. Samples processed for ChIP were diluted 1:1 with 2X RIPA buffer (280mM NaCl + 20mM HEPES + 2mM EDTA + 2% Glycerol + 2% TritonX100 + 0.2% Sodium Deoxycholate). Samples were incubated overnight with Rabbit anti-H3K27me3 (1μg, Millipore#07–449), Rabbit anti-histone H3

(0.5μg, Abcam#ab1791), or normal rabbit IgG (1μg, Cell Signaling Technology#2729). Antibody bound chromatin was pulled down for 4 hrs. with Protein A Agarose (Roche), washed 4 times with 1X RIPA and 1 time in in TE (10mM Tris + 1mM EDTA). Chromatin was then eluted twice in elution buffer (1% SDS + 0.1M $NaHCO_3$), first at room temperature and then at 55°C. Input samples were brought to the same volume with elution buffer and all samples were placed at 65°C overnight to reverse crosslinking. Each sample was then treated for 3hr with 20μg of Proteinase K at 55°C and the DNA purified by phenol/chloroform extraction, ethanol precipitation, and resuspension in TE.

Immunoprecipitated DNA was analyzed by Real-time qPCR using HotStart-IT SYBR Green qPCR Master Mix 2× (Affymetrix) on an Applied Biosystems 7300 RT-PCR System. PCR was performed in duplicates, which were averaged. In all graphs the immune-precipitated material is presented as a percentage of the DNA present in the input material. Primers used for PCR are described in Fig. 3A and Table S7 and were selected according to the protocol described in Braveman et al. (*73*).

Measurement of PRE excision efficiency

>UZ$^{\Delta PRE}$ clones were induced in larvae heterozygous for the *>PRE>UZ* transgene by a single, 60 min heat shock at 38°C at ~ 24, 48 or 72 hours before the end of larval life, as described for the ChIP-qPCR experiments in Fig. 3C. DNA was then extracted from wing discs of late third instar larvae (116–120 hr AEL) and analyzed by qPCR together in parallel with control DNAs extracted from wing discs of entirely *>UZ*$^{\Delta PRE}$ and *>PRE>UZ* larvae, using EX and IN probe pairs as in Fig. 3C.

Quantification of clone size

Larvae heterozygous for an *Act5c>Draf*$^{+}$*>lacZ* transgene (26) were given a weak heat shock (32.5°C for 1 hour) to ensure single *Act5c>lacZ*$^{\Delta Draf+}$clones could be identified. Notum clones were scored between the outer ring (wing hinge) and notum stripe of Wg staining and wing clones were scored within the inner ring of Wg, as indicated in Fig. S4. Clones were counted if at least half of the labeled clone nuclei resided within the designated region. The ImageJ Cell Counter tool was used to ensure that nuclei were only counted once.

Supplementary Material

Refer to Web version on PubMed Central for supplementary material.

Acknowledgments

We thank Mariann Bienz and Tulsi Patel for early help with assessing the *>EE>UZ* and *>PRE>UZ* transgenes, Atsuko Adachi and Chunyao Tao for technical assistance, and Jürg Müller, Mark Ptashne, K. Struhl, Richard Mann and Iva Greenwald for advice and discussion. Funding: HHMI Investigatorship, NIH R01 GM113000, Ellison Medical Foundation Senior Scholar Award AG-SS-2923-11; NIH Training grants 5T32GM007088 and T32DK07328; Bloomington stock center grant NIH P40OD018537.

References and Notes

1. Ptashne M. Principles of a switch. Nat Chem Biol. 2011; 7:484–487. [PubMed: 21769089]

2. Alon, U. An Introduction to Systems Biology: Design Principles of Biological Circuits. Chapman & Hall/CRC Press/Taylor & Fracis; Boca Raton, FL: 2006.
3. Moazed D. Mechanisms for the inheritance of chromatin states. Cell. 2011; 146:510–518. [PubMed: 21854979]
4. Steffen PA, Ringrose L. What are memories made of? How Polycomb and Trithorax proteins mediate epigenetic memory. Nature Reviews Molecular Cell Biology. 2014; 15:340–356. [PubMed: 24755934]
5. Bonasio R, Tu S, Reinberg D. Molecular signals of epigenetic states. Science (New York, NY). 2010; 330:612–616.
6. Margueron R, Reinberg D. The Polycomb complex PRC2 and its mark in life. Nature. 2011; 469:343–349. [PubMed: 21248841]
7. Lewis EB. A gene complex controlling segmentation in Drosophila. Nature. 1978; 276:565–570. [PubMed: 103000]
8. Struhl G. A gene product required for correct initiation of segmental determination in Drosophila. Nature. 1981; 293:36–41. [PubMed: 7266657]
9. Struhl G, Brower D. Early role of the esc+ gene product in the determination of segments in Drosophila. Cell. 1982; 31:285–292. [PubMed: 7159925]
10. Struhl G, Akam M. Altered distributions of Ultrabithorax transcripts in extra sex combs mutant embryos of Drosophila. The EMBO Journal. 1985; 4:3259–3264. [PubMed: 2419125]
11. Cao R, et al. Role of histone H3 lysine 27 methylation in Polycomb-group silencing. Science. 2002; 298:1039–1043. [PubMed: 12351676]
12. Czermin B, et al. Drosophila enhancer of Zeste/ESC complexes have a histone H3 methyltransferase activity that marks chromosomal Polycomb sites. Cell. 2002; 111:185–196. [PubMed: 12408863]
13. Kuzmichev A, Nishioka K, Erdjument-Bromage H, Tempst P, Reinberg D. Histone methyltransferase activity associated with a human multiprotein complex containing the Enhancer of Zeste protein. Genes Dev. 2002; 16:2893–2905. [PubMed: 12435631]
14. Müller J, et al. Histone methyltransferase activity of a Drosophila Polycomb group repressor complex. Cell. 2002; 111:197–208. [PubMed: 12408864]
15. McKay, Daniel J., et al. Interrogating the Function of Metazoan Histones using Engineered Gene Clusters. Developmental Cell. 2015; 32:373–386. [PubMed: 25669886]
16. Pengelly AR, Copur O, Jackle H, Herzig A, Muller J. A Histone Mutant Reproduces the Phenotype Caused by Loss of Histone-Modifying Factor Polycomb. Science. 2013; 339:698–699. [PubMed: 23393264]
17. Chan CS, Rastelli L, Pirrotta V. A Polycomb response element in the Ubx gene that determines an epigenetically inherited state of repression. EMBO J. 1994; 13:2553–2564. [PubMed: 7912192]
18. Christen B, Bienz M. Imaginal disc silencers from Ultrabithorax: evidence for Polycomb response elements. Mechanisms of development. 1994; 48:255–266. [PubMed: 7893606]
19. Simon J, Chiang A, Bender W, Shimell MJ, O'Connor M. Elements of the Drosophila bithorax complex that mediate repression by Polycomb group products. Dev Biol. 1993; 158:131–144. [PubMed: 8101171]
20. Henikoff S, Shilatifard A. Histone modification: cause or cog? Trends Genet. 2011; 27:389–396. [PubMed: 21764166]
21. Zhu B, Reinberg D. Epigenetic inheritance: uncontested? Cell Res. 2011; 21:435–441. [PubMed: 21321606]
22. Ptashne, M. Proceedings of the National Academy of Sciences. Vol. 110. National Acad Sciences; 2013. p. 7101-7103.
23. Henikoff S, Greally JM. Epigenetics, cellular memory and gene regulation. Current biology. 2016; CB26:R644–648.
24. Pirrotta V, Chan CS, McCabe D, Qian S. Distinct parasegmental and imaginal enhancers and the establishment of the expression pattern of the Ubx gene. Genetics. 1995; 141:1439–1450. [PubMed: 8601485]

25. Bienz M, Muller J. Transcriptional silencing of homeotic genes in Drosophila. Bioessays. 1995; 17:775–784. [PubMed: 8763830]
26. Struhl G, Basler K. Organizing activity of wingless protein in Drosophila. Cell. 1993; 72:527–540. [PubMed: 8440019]
27. Busturia A, Wightman CD, Sakonju S. A silencer is required for maintenance of transcriptional repression throughout Drosophila development. Development. 1997; 124:4343–4350. [PubMed: 9334282]
28. Sengupta AK, Kuhrs A, Müller J. General transcriptional silencing by a Polycomb response element in Drosophila. Development. 2004; 131:1959–1965. [PubMed: 15056613]
29. Mann RS, Morata G. The developmental and molecular biology of genes that subdivide the body of Drosophila. Annu Rev Cell Dev Biol. 2000; 16:243–271. [PubMed: 11031237]
30. Beuchle D, Struhl G, Müller J. Polycomb group proteins and heritable silencing of Drosophila Hox genes. Development. 2001; 128:993–1004. [PubMed: 11222153]
31. Oktaba K, et al. Dynamic regulation by polycomb group protein complexes controls pattern formation and the cell cycle in Drosophila. Dev Cell. 2008; 15:877–889. [PubMed: 18993116]
32. Birve A, et al. Su(z)12, a novel Drosophila Polycomb group gene that is conserved in vertebrates and plants. Development. 2001; 128:3371–3379. [PubMed: 11546753]
33. Anderson PR, Kirby K, Hilliker AJ, Phillips JP. RNAi-mediated suppression of the mitochondrial iron chaperone, frataxin, in Drosophila. Hum Mol Genet. 2005; 14:3397–3405. [PubMed: 16203742]
34. Caceres L, et al. Nitric oxide coordinates metabolism, growth, and development via the nuclear receptor E75. Genes Dev. 2011; 25:1476–1485. [PubMed: 21715559]
35. Basler K, Struhl G. Compartment boundaries and the control of Drosophila limb pattern by hedgehog protein. Nature. 1994; 368:208–214. [PubMed: 8145818]
36. Alabert C, et al. Two distinct modes for propagation of histone PTMs across the cell cycle. Genes Dev. 2015; 29:585–590. [PubMed: 25792596]
37. Gaydos LJ, Wang W, Strome S. H3K27me and PRC2 transmit a memory of repression across generations and during development. Science. 2014; 345:1515–1518. [PubMed: 25237104]
38. Xu M, Wang W, Chen S, Zhu B. A model for mitotic inheritance of histone lysine methylation. EMBO Rep. 2012; 13:60–67.
39. Papp B, Müller J. Histone trimethylation and the maintenance of transcriptional ON and OFF states by trxG and PcG proteins. Genes Dev. 2006; 20:2041–2054. [PubMed: 16882982]
40. Martín FA, Herrera SC, Morata G. Cell competition, growth and size control in the Drosophila wing imaginal disc. Development (Cambridge, England). 2009; 136:3747–3756.
41. Gunesdogan U, Jackle H, Herzig A. A genetic system to assess in vivo the functions of histones and histone modifications in higher eukaryotes. EMBO Rep. 2010; 11:772–776. [PubMed: 20814422]
42. McGuire SE, Le PT, Osborn AJ, Matsumoto K, Davis RL. Spatiotemporal Rescue of Memory Dysfunction in Drosophila. Science. 2003; 302:1765–1768. [PubMed: 14657498]
43. Ptashne M. Epigenetics: core misconcept. Proc Natl Acad Sci U S A. 2013; 110:7101–7103. [PubMed: 23584020]
44. Henikoff, S., Greally, JM. Curr Biol. Vol. 26. Elsevier; 2016. p. R644-R648.
45. Zhang CC, Bienz M. Segmental determination in Drosophila conferred by hunchback (hb), a repressor of the homeotic gene Ultrabithorax (Ubx). Proc Natl Acad Sci USA. 1992; 89:7511–7515. [PubMed: 1354356]
46. Margueron R, et al. Role of the polycomb protein EED in the propagation of repressive histone marks. Nature. 2009; 461:762–767. [PubMed: 19767730]
47. Jiao, L., Liu, X. Science. Vol. 350. American Association for the Advancement of Science; 2015. p. aac4383-aac4383.
48. Justin N, et al. Nature Communications. 2016; 7:11316.
49. Steffen PA, et al. Quantitative in vivo analysis of chromatin binding of Polycomb and Trithorax group proteins reveals retention of ASH1 on mitotic chromatin. Nucleic Acids Res. 2013; 41:5235–5250. [PubMed: 23580551]

50. Fischle W, et al. Molecular basis for the discrimination of repressive methyl-lysine marks in histone H3 by Polycomb and HP1 chromodomains. Genes & Development. 2003; 17:1870–1881. [PubMed: 12897054]
51. Min J, Zhang Y, Xu RM. Structural basis for specific binding of Polycomb chromodomain to histone H3 methylated at Lys 27. Genes & Development. 2003; 17:1823–1828. [PubMed: 12897052]
52. Simon JA, Kingston RE. Occupying chromatin: polycomb mechanisms for getting to genomic targets, stopping transcriptional traffic, and staying put. Molecular cell. 2013; 49:808–824. [PubMed: 23473600]
53. Schwartz YB, et al. Genome-wide analysis of Polycomb targets in Drosophila melanogaster. Nat Genet. 2006; 38:700–705. [PubMed: 16732288]
54. Copur O, Muller J. The histone H3-K27 demethylase Utx regulates HOX gene expression in Drosophila in a temporally restricted manner. Development. 2013; 140:3478–3485. [PubMed: 23900545]
55. Deal RB, Henikoff JG, Henikoff S. Genome-wide kinetics of nucleosome turnover determined by metabolic labeling of histones. Science. 2010; 328:1161–1164. [PubMed: 20508129]
56. Mito Y, Henikoff JG, Henikoff S. Genome-scale profiling of histone H3.3 replacement patterns. Nat Genet. 2005; 37:1090–1097. [PubMed: 16155569]
57. Petruk S, et al. TrxG and PcG Proteins but Not Methylated Histones Remain Associated with DNA through Replication. Cell. 2012
58. Lanzuolo C, Lo Sardo F, Diamantini A, Orlando V. PcG complexes set the stage for epigenetic inheritance of gene silencing in early S phase before replication. PLoS genetics. 2011; 7:e1002370. [PubMed: 22072989]
59. Bintu L, et al. Dynamics of epigenetic regulation at the single-cell level. Science. 2016; 351:720–724. [PubMed: 26912859]
60. Hansen KH, et al. A model for transmission of the H3K27me3 epigenetic mark. Nat Cell Biol. 2008; 10:1291–1300. [PubMed: 18931660]

One Sentence Summary

Inheritance of H3K27me3 nucleosomes constitutes the molecular basis for epigenetic silencing of a Drosophila HOX gene.

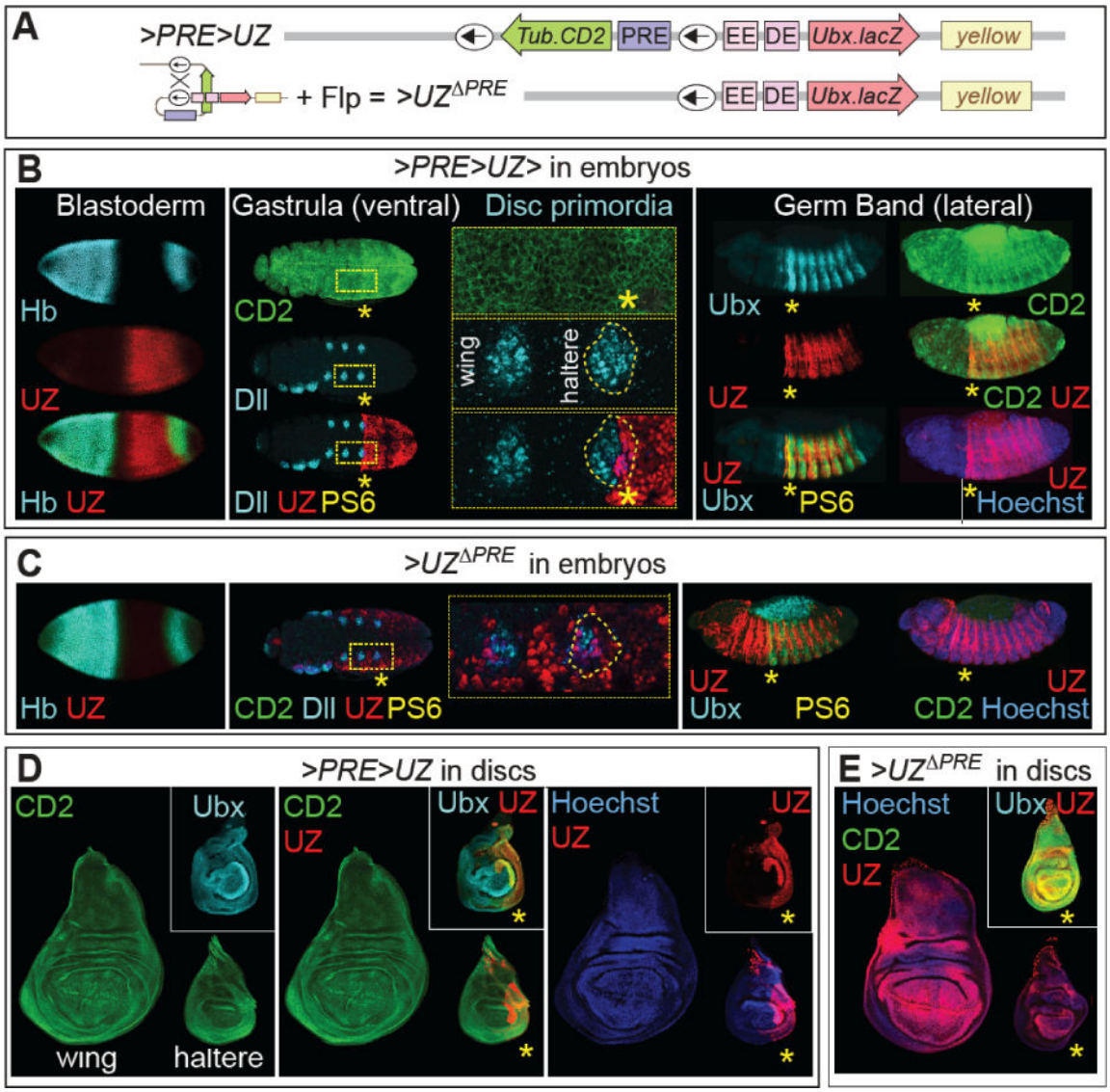

Figure 1. Role of the PRE in establishing ON and OFF states of the *>PRE>UZ* transgene

(A) Structure of *>PRE>UZ* and *>UZ*$^{\Delta PRE}$ transgenes. The *Ubx* promoter drives expression of the *lacZ* coding sequence (red; arrow points in the direction of transcription) and is regulated by the PRE, an early enhancer (EE) and a disc enhancer (DE) (Methods). The PRE is embedded in a Flp-out cassette flanked by Flp recombinase target (FRT) sequences (encircled arrows) and contains a *Tub.CD2* marker gene transcribed in the opposite direction (green). The transgene is marked by a *yellow*$^{+}$ mini-gene. (B) *Ubx.lacZ* (UZ, red) and *Tub.CD2* (CD2 green) expression from the *>PRE>UZ* transgene. UZ is first apparent in a central domain of blastoderm stage embryos delimited by the transcription factor Hunchback (Hb; turquoise), which represses EE enhancer activity, after which it is heritably ON in parasegments 6–12 and OFF in the remaining parasegments (gastrula and late stage germ band embryos). The gastrula image shows the three left-right pairs of the thoracic disc primordia, as well as three gnathal primordia on the lower side (marked by Distalless, Dll, turquoise). The wing and haltere primordia on one side are boxed and shown at higher

magnification (here and elsewhere, anterior is to the left, parasegment 6 is indicated by a yellow asterisk and Hoechst (DNA; blue) provides a counterstain). The anterior boundary of UZ coincides with the anterior boundary of parasegment 6, which subdivides the haltere primordium into anterior (A) and posterior (P) compartments. CD2 is also transiently up-regulated in parasegments 6–12 at this stage (only parasegment 6 and 7 are apparent in this image). UZ expression in late germ band embryos closely resembles that of native Ubx (turquoise). (C) UZ expression in embryos carrying the *>UZ$^{\Delta PRE}$* transgene (stained as in B; absence of the *>PRE>* cassette is confirmed by the absence of CD2). UZ is not expressed at the blastoderm stage but comes on ubiquitously after gastrulation. (D) UZ expression in third instar wing and haltere discs carrying the *>PRE>UZ* transgene; the insert shows a haltere disc independently stained for UZ and Ubx. UZ is ON in the P compartment of the haltere but OFF in the A compartment as well as in the entire wing disc; CD2 expression is uniform. Native Ubx is ON in the entire haltere disc but does not over-ride the OFF state of the *>PRE>UZ* transgene in the A compartment. (E) UZ expression in wing and haltere discs carrying the *>UZ$^{\Delta PRE}$* transgene. UZ is expressed in all cells, albeit with stereotyped, position-dependent differences in level that correlate with the kinetics of release from silencing following PRE excision (Fig. 2).

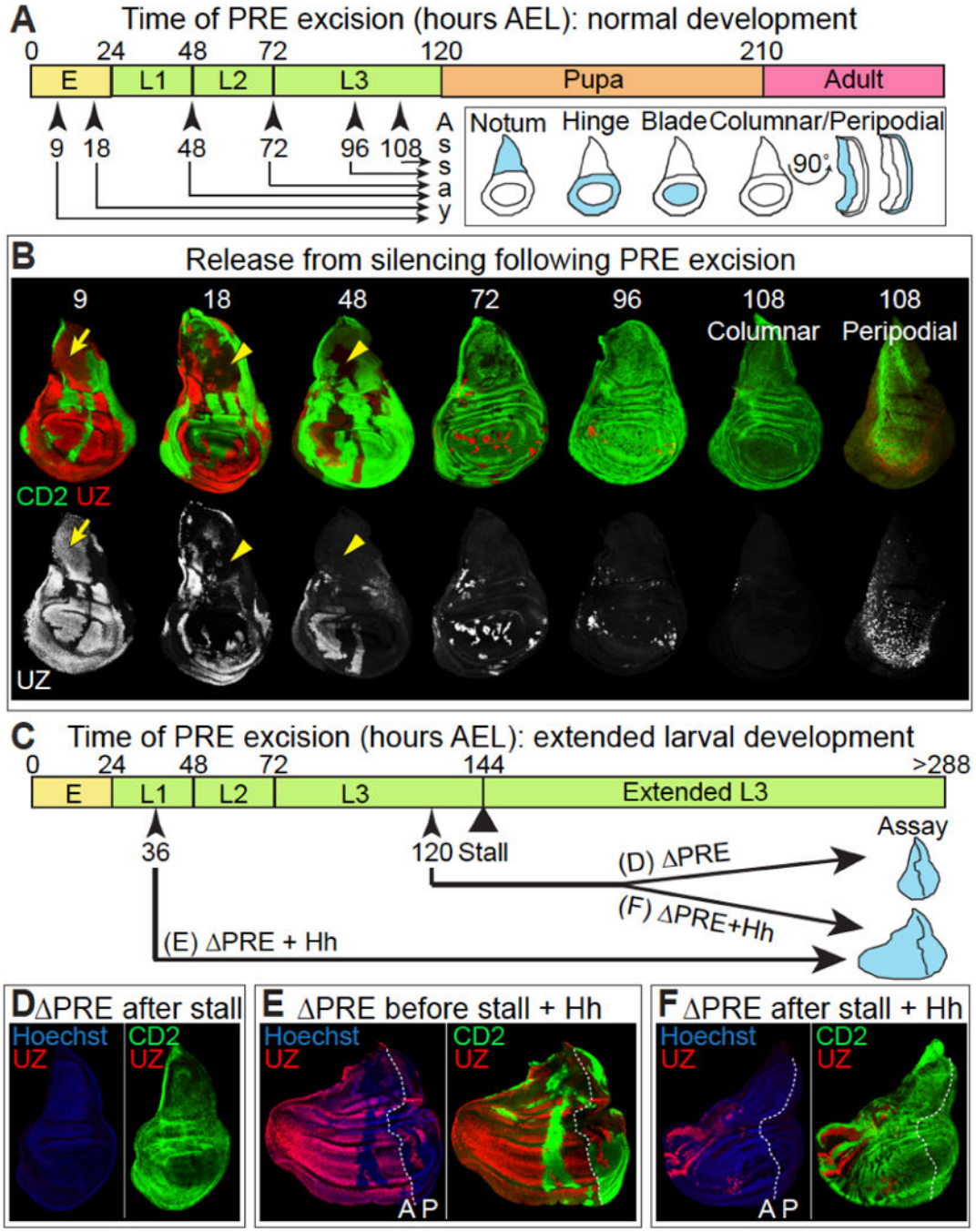

Figure 2. Release from silencing following >*PRE*> excision depends on cell position and number of cell divisions

(A) Schedule of induction of *>UZ$^{\Delta PRE}$* clones (E = embryo; L1, 2 and 3 = first, second and third larval instars; AEL, time after egg laying (in hours). For all time points (arrow heads), clones were assayed in mature wing discs at the end of larval life (~120 AEL; inset shows the prospective notum (body wall), hinge, and wing blade domains of the columnar epithelium, as well as the peripodial epithelium). (B) Wing discs carrying the *>PRE>UZ* transgene stained for UZ (red top, white bottom) and CD2 (green, top) following *>PRE>* excision at the time points indicated. The columnar epithelium is shown for all discs, and the

peripodial epithelium is also shown for the 108 AEL disc. *>UZ$^{\Delta PRE}$* clones are marked "black" by the absence of CD2 expression. Most clones induced in mid-stage embryos (9 AEL) cell-autonomously derepress UZ (e.g., arrow). However, clones induced later derepress UZ in a manner that depends on position within the disc and the time of clone induction (e.g., 18 and 48 AEL clones fail to derepress UZ, respectively, in most or all of the notum (arrowheads); 72 and 96 AEL clones fail to show release from silencing in most of the prospective notum, wing hinge, and some regions of the wing blade; and 108 AEL clones show release only in peripodial cells). (C) Schedule of induction of *>UZ$^{\Delta PRE}$* clones in "stalled" wing discs (Methods). In this background, cell division ceases when the imaginal discs reach full size at around 144 AEL, while larvae continue to feed and grow for up to three weeks. Arrowheads indicate the timing of *>PRE>* excision in the presence (E,F) or absence (D) of co-induced *Tub>hh* clones. (D) Stalled wing disc two weeks after *>PRE>* excision at 120AEL (stained as in B): no UZ expression is detected despite *>PRE>* excision having occurred two weeks previously (clones are not apparent at this magnification, having undergone only one or two divisions before the stall). (E) Stalled wing disc heat shocked to co-induce *>UZ$^{\Delta PRE}$* and *Tub>hh* clones during the first larval instar (24–48 AEL), assayed ~one week later. Large clonal patches are apparent in both the A and P compartments (the patches in A are exceptionally large owing to the extra growth induced by ectopic Hh). UZ is expressed throughout the clones located within the prospective wing blade. (F) Stalled wing disc heat shocked to co-induce *>UZ$^{\Delta PRE}$* and *Tub>hh* clones ~ 24 hrs before the stall and assayed ~2 weeks later. Clones in the A compartment continue to proliferate as a function of distance from the A/P boundary: clones located far from the A/P boundary are large and de-repress UZ throughout the prospective wing, whereas clones closer to the A/P boundary are smaller and show release from silencing in the vicinity of the D/V boundary (as in 96 AEL clones in B). In contrast, clones in the remainder of the disc (posterior A and the entirety of P) stop dividing after only a few divisions and do not express UZ. Excision clones displayed in this figure were induced by a 1 hr heat shock at 36±1°C.

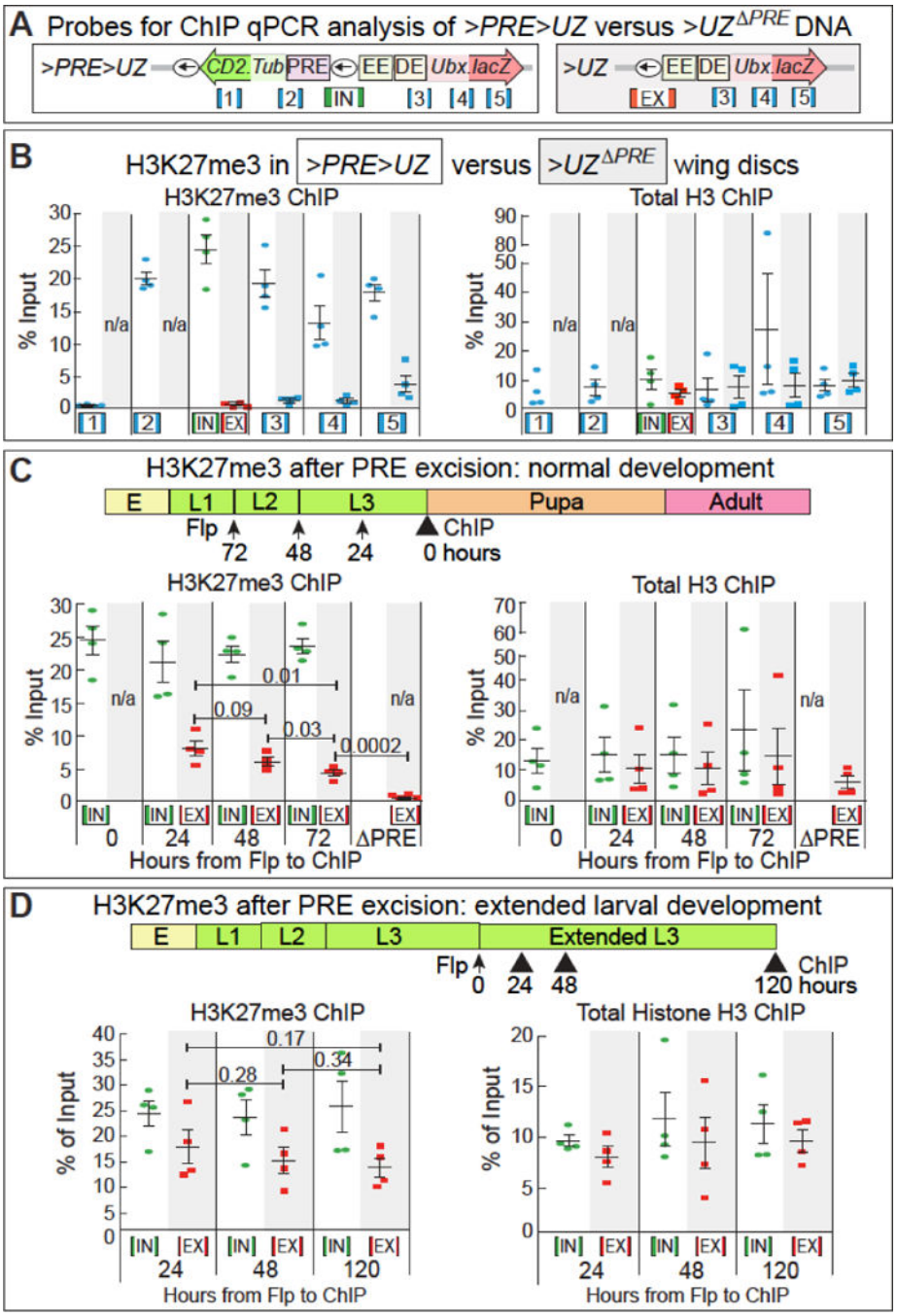

Figure 3. Cell division-dependent dilution of H3K27me3 following PRE excision

(A) Probe pairs used for ChIP-qPCR of H3K27me3 and total H3 associated with the *>PRE>UZ* and *>UZ*$^{\Delta PRE}$ transgenes (all probe pairs detect only DNA in the transgene and not endogenous *Ubx* or *Tub* DNA, and are indicated as blue, green or red segments with the amplified regions shown as white segments; not to scale; Table S7). (B) ChIP-qPCR for H3K27me3 and total H3 for entirely *>PRE>UZ* (white) and *>UZ*$^{\Delta PRE}$ (grey) wing discs (120 AEL). H3K27me3 is detected for all of the probed regions of *>PRE>UZ* except for the ubiquitously expressed, CD2 encoding region amplified by probe pair #1. In contrast, no

significant H3K27me3 signal was observed for any of probed regions for the *>UZ$^{\Delta PRE}$* transgene (total H3 levels were similar for all probed segments for both transgenes; here and elsewhere, see the indicated Table (Table S1 in this case) for detailed quantitation and mock ChIP controls). (C) ChIP-qPCR analysis of H3K27me3 following PRE excision during normal development. The schedule is shown at the top (as in Fig. 2B). ChIP-qPCR data are shown for "IN" probes, which detect only intact *>PRE>UZ* DNA (white columns, green) and "EX" probes, which detect only *>UZ$^{\Delta PRE}$* DNA (grey columns, red). The experimental design does not allow a meaningful "zero" time point for H3K27me3 associated with *>UZ$^{\Delta PRE}$* DNA immediately following PRE excision. Comparing the change in H3K27me3 between the 24–48, 48–72 and 24–72 time points, the EX probe data indicate a decline in H3K27me3 levels of ~10–12%/cell cycle for both the 24–48 and 48–72 hr time points, normalized by direct assessment of cell division in parallel experiments (Fig. S4); total H3 remained constant. H3K27me3 after 72 hours is still significantly above background, as monitored in the *>UZ$^{\Delta PRE}$* control. No significant change is detected by the IN probes for H3K27me3 or total H3 (Table S2). (D) ChIP-qPCR analysis of H3K27me3 following PRE excision in "stalled discs" during extended larval development. *>UZ$^{\Delta PRE}$* clones were induced around the time of the stall and assayed by ChIP-qPCR at 24, 48 and 120 hours afterwards (top, as in Fig. 2D). No significant change was observed in H3K27me3 or total H3 using the same probes as in C, even after 120 hrs (Table S3). Here, and in Figs. 4A and 5B, each data point indicates the percent input value for a single biological replicate and bars represent the mean±SEM of 4 independent replicates. Values above plots represent P values calculated by unpaired *t* test. "n/a" signifies that the DNA is not present for detection in the *>UZ$^{\Delta PRE}$* genotype. *>UZ$^{\Delta PRE}$* clones in C and D were induced by 1 hr heat shock at 38°C.

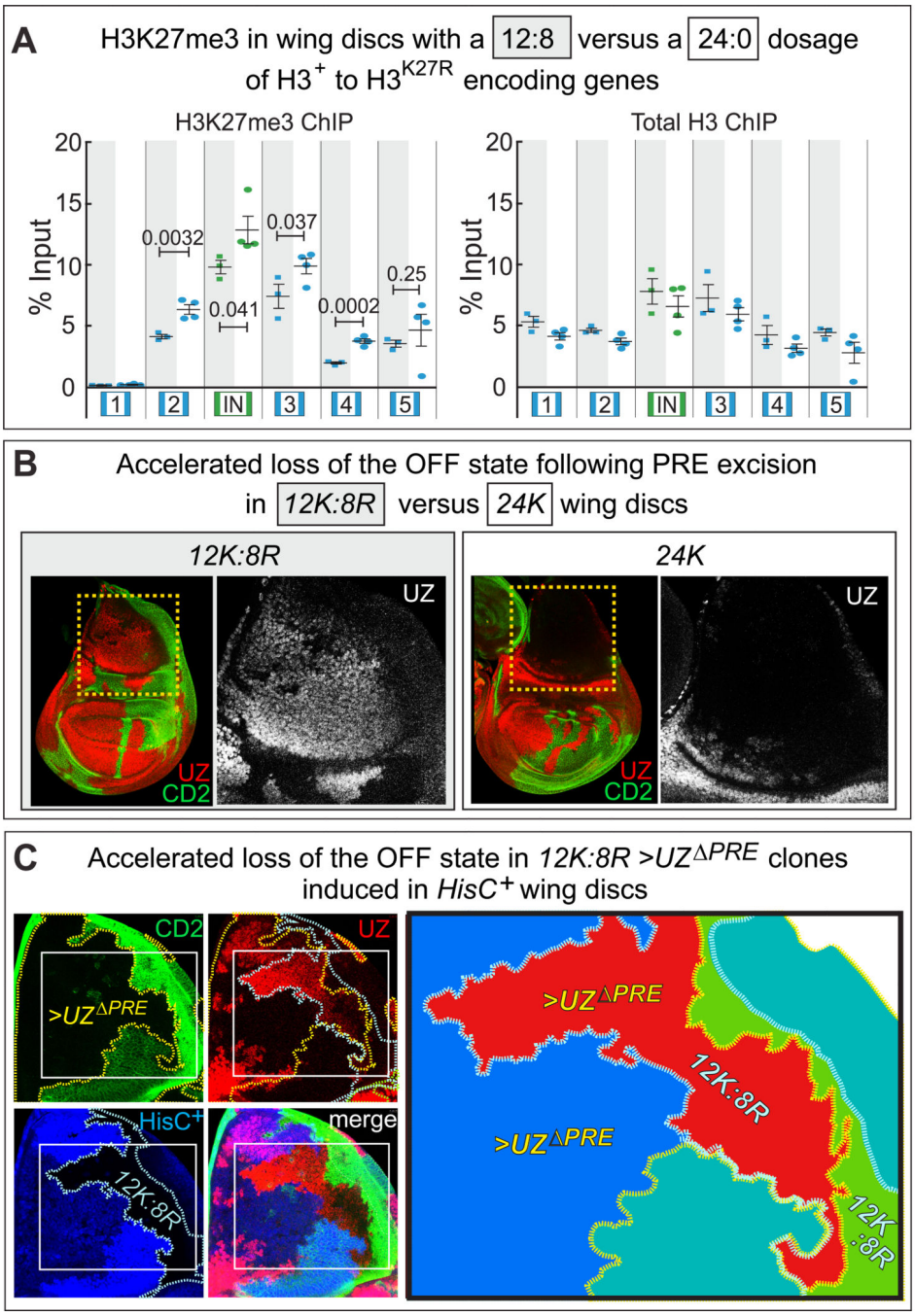

Figure 4. Spiking the H3^{+} pool with H3^{K27R} reduces H3K27me3 and accelerates loss of the OFF state

(A) ChIP-qPCR analysis of the *>PRE>UZ* transgene in wing discs in which the native histone gene complex is replaced by transgenes expressing 12 copies of the H3^{+} coding sequence plus 8 copies of the H3^{K27R} coding sequence (12K:8R; grey; probes as in Fig. 3A), or alternatively, by transgenes containing 24 copies of the H3^{+} coding sequence (24K; white; Methods). For each of the five probed regions that are H3K27 trimethylated in wild type wing discs (Fig. 3B), H3K27me3 is reduced by ~30–40% comparing 12K:8R to 24K discs (no significant difference is seen total H3 ChIP; Table S4). (B) Mature 12K:8R or 24K wing

discs carrying multiple *>UZ$^{\Delta PRE}$* clones induced during the first larval instar (marked by the absence of CD2). In 24K discs (right panel), as in wild type discs (Fig. 2B), *>UZ$^{\Delta PRE}$* clones remains silenced in the prospective notum (boxed in yellow; magnified to the right). In 12K:8R discs (left panel), *>UZ$^{\Delta PRE}$* clones show extensive release from silencing. (C) The prospective notum of a 12K:8R wing disc carrying the *>PRE>UZ* transgene as well as a single copy of the native Histone gene complex (*HisC^{+}*), and in which three kinds of clones have been co-induced during the first larval instar: (i) *>UZ$^{\Delta PRE}$* clones in which the transgene PRE has been excised, but *HisC^{+}* remains present (blue in the cartoon; marked "black" in the upper left image by the absence of CD2, green, and blue in the lower left image by the presence of a *Ubi.GFP* transgene linked in cis to the single *HisC^{+}* allele); (ii) *12K:8R* clones that retain the intact *>PRE>UZ* transgene but have lost *HisC^{+}* (green in the cartoon; marked green in the upper left image and "black" in the lower left image); and (iii) *>UZ$^{\Delta PRE}$ 12K:8R* clones that have lost both the PRE and *HisC^{+}* (red in the cartoon, marked black in the upper and lower left images); cell populations that retain both the PRE and *HisC^{+}* are shown as turquois in the cartoon. Only the *>UZ$^{\Delta PRE}$ 12K:8R* clones express UZ in the central portion of the notum (red), whereas the remaining two kinds of clones do not. Clones in B and C were induced by 1 hr heat shock at 37.5°C.

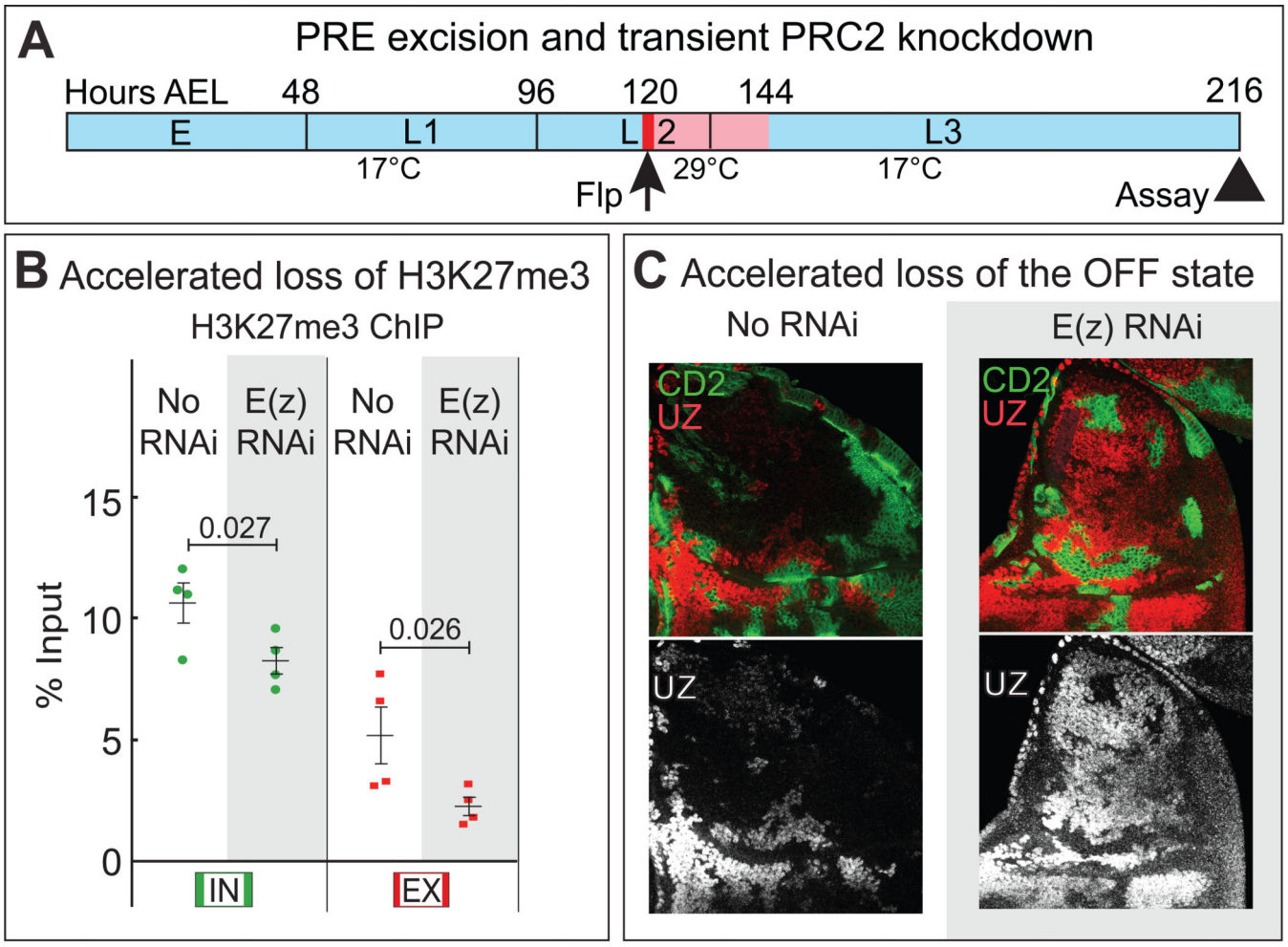

Figure 5. Transient reduction in PRC2 activity accelerates loss of H3K27me3 and the OFF state

(A) Schedule of induction of *>UZ*$^{\Delta PRE}$ clones (generated by a one hour heat shock at 37°C; dark red) followed by a transient loss of PRC2 activity (24 hours, 29°C light red) relative to larval instars at 17°C. Transient loss of PRC2 was achieved by RNAi knock-down of E(z), the catalytic subunit of PRC2, under Gal80^{ts}/Gal4 control, which allows normal PRC2 activity at 17°C, but reduces or abolishes it at 29°C. **(B)** H3K27me3 ChIP-qPCR was performed using EX and IN probes, which assay the PRE deleted (*>UZ*) and intact (*>PRE>UZ*) transgenes (as in Fig. 3A; Table S5). RNAi (experimental) and no RNAi (control) discs were analyzed in strict parallel. Transient RNAi knock-down of PRC2 following PRE excision causes a 2.5 fold further decrease in H3K27me3 relative to the control (EX probe), in contrast to a modest 20% reduction in H3K27me3 observed in cells that did not excise the PRE (IN probe). (C) UZ expression in the notum region of no RNAi and E(z) RNAi wing discs, stained for UZ (red/white) and CD2 (green); *>UZ*$^{\Delta PRE}$ clones are marked by the absence of CD2. Extensive UZ expression is observed in *>UZ*$^{\Delta PRE}$ clones in E(z) RNAi discs, in contrast to sporadic, weak expression in control discs. *>UZ*$^{\Delta PRE}$ clones in B and C were induced by 1 hr heat shock at 38°C.

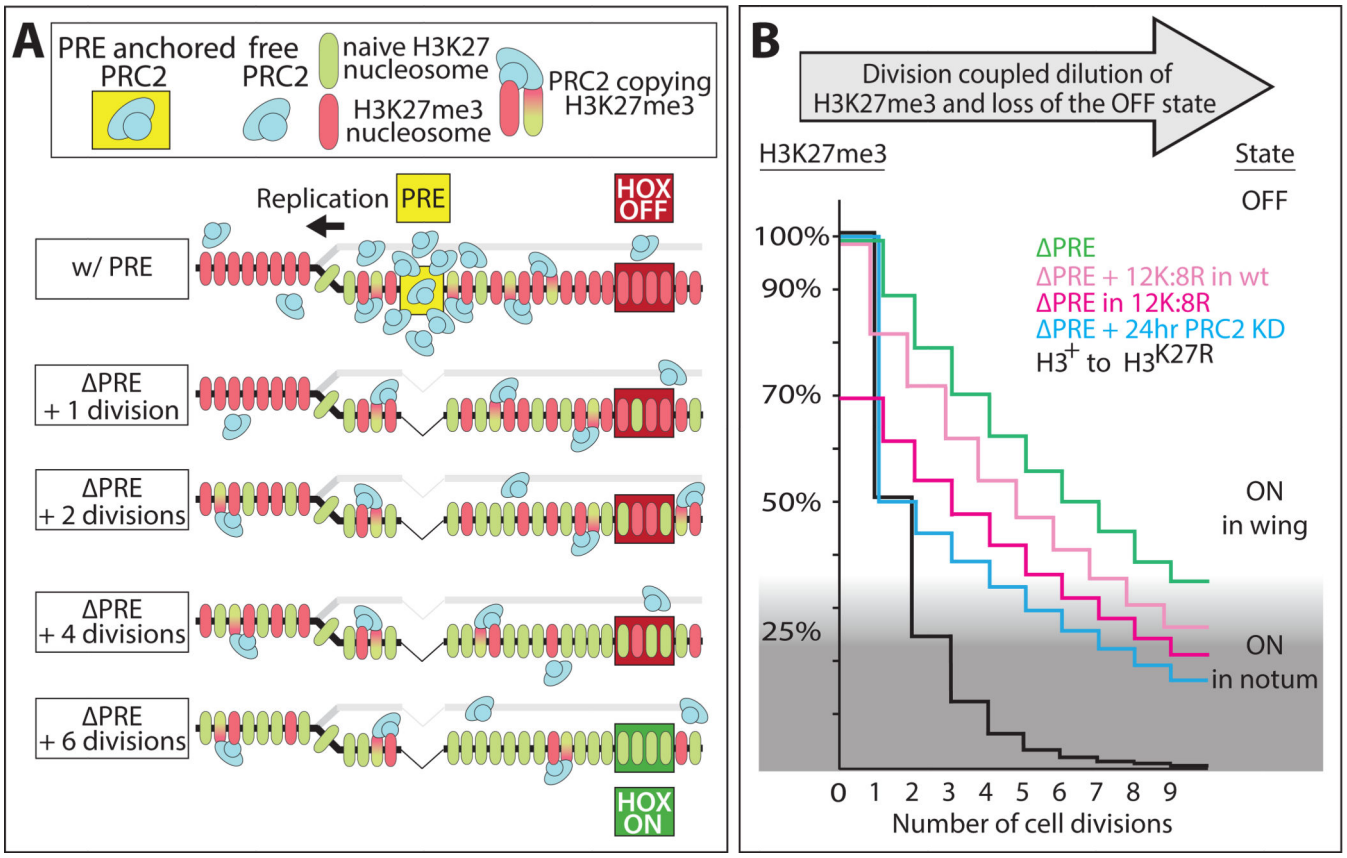

Figure 6. Epigenetic memory of the OFF state by inheritance of H3K27me3

(A) The model.

Maintenance of the OFF state of silenced HOX loci depends on H3K27me3 catalyzed by the Polycomb Repressive Complex 2 (PRC2), recruited by cis-acting Polycomb Response Elements (PREs). Following replication, parental H3K27me3 nucleosomes are efficiently re-deposited at the HOX locus, but diluted by half by incorporation of newly synthesized, naive nucleosomes; PRC2 is induced by binding to H3K27me3 on parental nucleosomes to copy the K27me3 mark onto neighboring, naïve nucleosomes (depicted only on the bottom daughter strand). Targeting of PRC2 to the PRE ("w/PRE") is required for efficient copying, and the process reiterates after each replication cycle, propagating the epigenetic memory of the OFF state without requiring additional inputs to perpetuate the state. Following PRE excision ("ΔPRE"), residual "free" PRC2 can copy the mark, but inefficiently, resulting in the serial dilution of H3K27me3 nucleosomes following each replication cycle, and the release from silencing when the level of H3K27me3 falls beneath a critical threshold.

(B) The evidence.

In otherwise wildtype cells, the rate of division-coupled dilution of H3K27me3 nucleosomes following PRE excision is slow (~10–12%/cell cycle; ΔPRE; green), indicating that sufficient PRC2 activity remains in the absence of the PRE to copy most of the H3K27me3 marks from parental nucleosomes to naïve nucleosomes. However, after sufficient divisions occur to dilute H3K27me3 nucleosomes below distinct thresholds, the memory of the OFF state is lost in a manner that depends on cell position, e.g., after ~4–6 divisions and a decline of >50% for cells located in the prospective wing (yellow) and after >8–9 divisions and a

decline of >75% for cells in the prospective notum (grey). Compromising the copying capacity of PRC2 further by introducing a sub-population of K27R mutant histone H3 molecules that cannot be trimethylated [either from fertilization onwards (ΔPRE in 12K:8R; dark pink) or concomitant with PRE excision (ΔPRE 12K:8R in wt; light pink)], or alternatively, by transiently knocking down free PRC2 activity (ΔPRE + 24 hr PRC2 KD, turquoise), causes a corresponding acceleration in both the dilution of H3K27 as well as the loss of the memory of the OFF state. Finally, in the extreme case in which the capacity of PRC2 to copy the mark is abruptly terminated by replacing all newly synthesized nucleosomes available for incorporation with the H3K27R mutant form ($H3^{+}$ to $H3^{K27R}$; black), silencing of the native *Ubx* gene is lost in a manner that correlates with the number of cell divisions and appears to obey the same region-specific thresholds for release from silencing as the *>PRE>UZ* transgene, assuming a 50% dilution of parental H3K27me3 nucleosomes following each round of replication. Collectively, these results establish a causal relationship between inheritance of H3K27me3 and the epigenetic memory of the OFF state.